Journal of Zhejiang University-SCIENCE A (Applied Physics & Engineering)

Emerging applicability of two-dimensional boron for energy catalysis

Dake ZHANG, Chengcheng ZHANG, Shenghua WANG, Wei SUN

Cite this as: Dake ZHANG, Chengcheng ZHANG, Shenghua WANG, Wei SUN, 2024. Emerging applicability of two-dimensional boron for energy catalysis. *Journal of Zhejiang University-SCIENCE A (Applied Physics & Engineering)*, 25(10):877-888. https://doi.org/10.1631/jzus.A2400003

Synthesis of 2D boron using top-down strategies

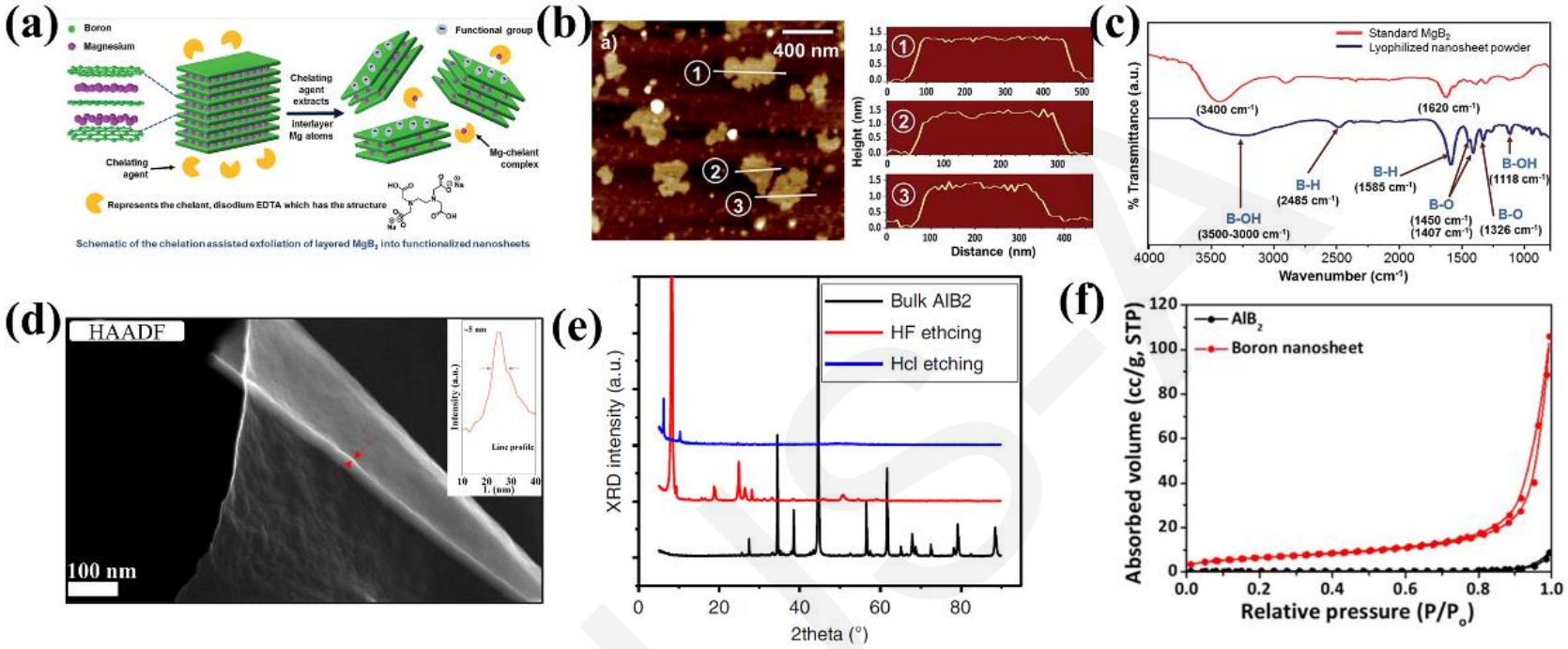


Fig. 1 (a) Schematic depicting the process of EDTA chelating a substantial fraction of interlayer Mg atoms. (b) AFM images of the obtained boron nanosheets. (c) Fourier-transform infrared spectroscopy (FT-IR) spectra of standard MgB_2 and boron nanosheets. (a-c) Reprinted from (James and Jasuja, 2017) (Copyright 2017, with permission from the Royal Society of Chemistry). (d) TEM image of the boron nanosheets. The inset image is the line profile at position "L". Reprinted from (Zhang, et al., 2024) (Copyright 2024, with permission from the Royal Society of Chemistry). (e) XRD patterns of bulk AlB_2, the boron product after HCl etching, and the aluminum product after HF etching. Reprinted from (Xie et al., 2022) (Copyright 2022, with permission from Springer Nature). (f) Nitrogen absorption-desorption isotherms of boron nanosheets and their precursor AlB_2. Reprinted from (Cai et al., 2022) (Copyright 2022, with permission from the Royal Society of Chemistry).

Synthesis of 2D boron using top-down strategies

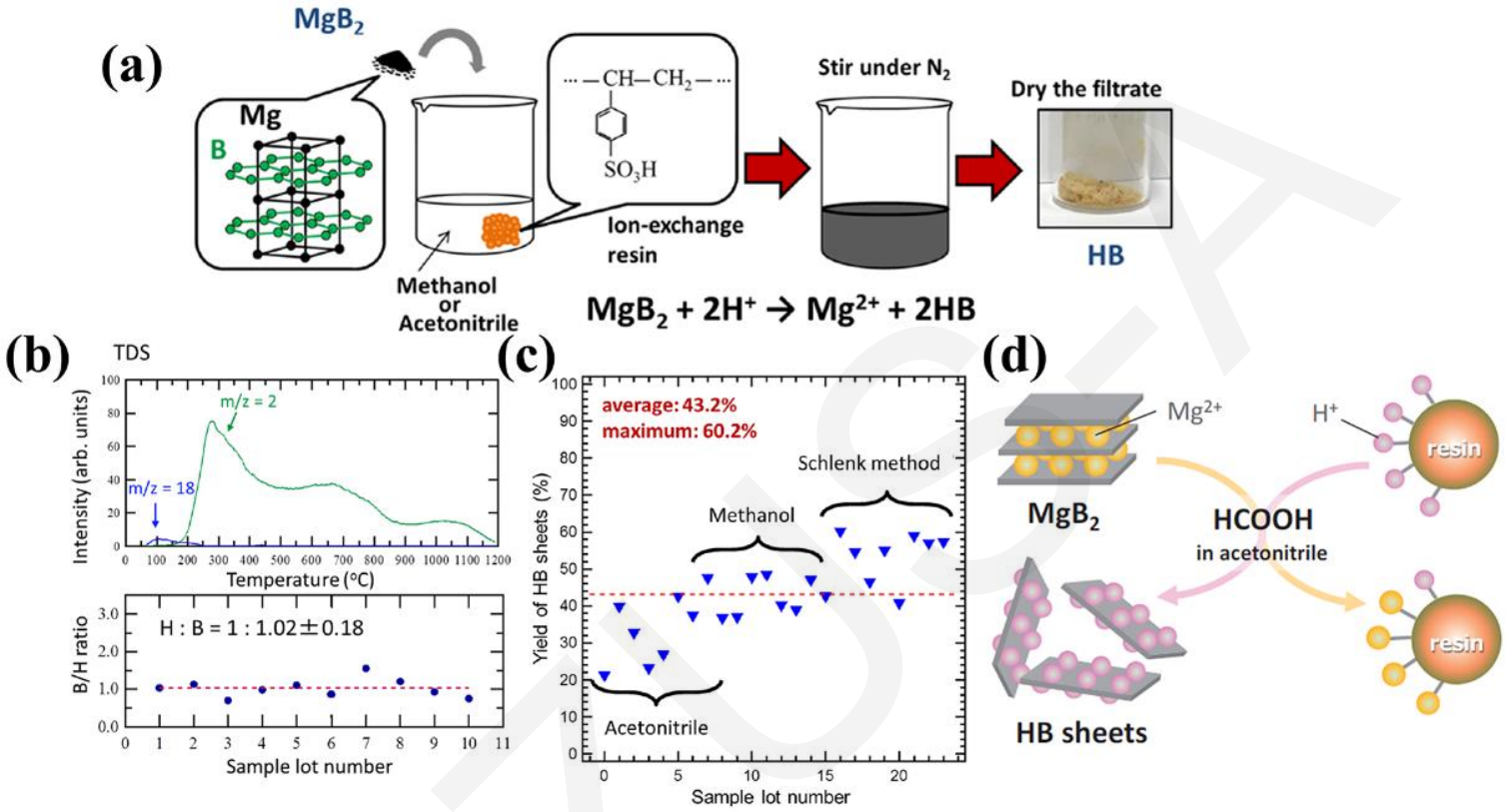


Fig. 2 (a) Schematic illustration of HB nanosheet preparation by a cation exchange process. (b) TDS of HB nanosheets. (a-b) Reprinted from (Nishino, et al., 2017a) (Copyright 2017, with permission from the American Chemical Society). (c) Yields of HB nanosheets using the conventional ion-exchange method with acetonitrile and methanol, and the Schlenk method with methanol. Reprinted from (Tominaka, et al., 2020) (Copyright 2020, with permission from Elsevier). (d) Schematic illustration of the synthesis of HB nanosheets facilitated by formic acid. Reprinted from (Kawamura, et al., 2020) (Copyright 2020, with permission from The Chemical Society of Japan).

Synthesis of 2D boron using top-down strategies

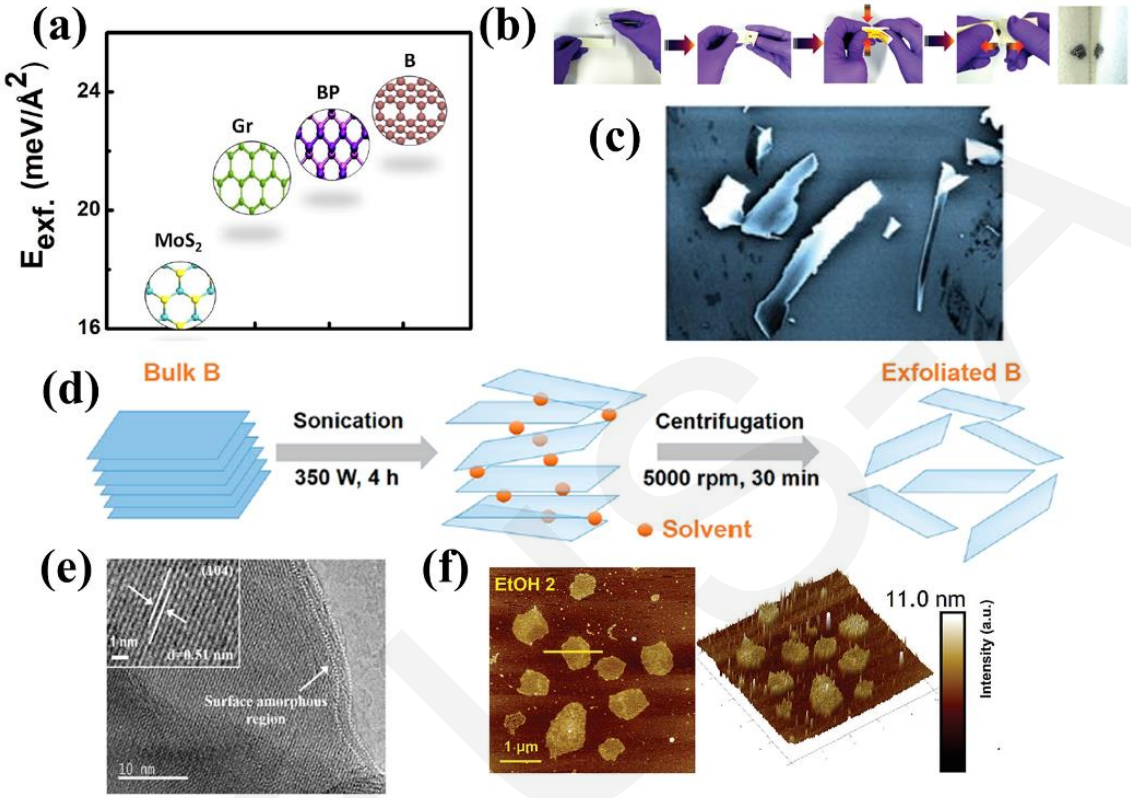


Fig. 3(a) Exfoliation energy of different materials (including MoS_2, Gr, BP, and B). (b) Digital images of the steps of the mechanical exfoliation of boron nanosheets using double-sided foam tape. (c) FESEM image of the obtained boron sheets. (a-c) Reprinted from (Chahal, et al., 2021) (Copyright 2021, with permission from Wiley). (d) Schematic illustration of the ultrasonication liquid exfoliation process. Reprinted from (Li et al., 2018) (Copyright 2018, with permission from the American Chemical Society). (e) HRTEM image of the exfoliated boron nanosheets. Reprinted from (Ma et al., 2020) (Copyright 2020, with permission from the Royal Society of Chemistry). (f) AFM image of the exfoliated boron nanosheets in ethanol solvent. Reprinted from (Chand et al., 2022) (Copyright 2022, with permission from Wiley).

2D boron as catalytic sites

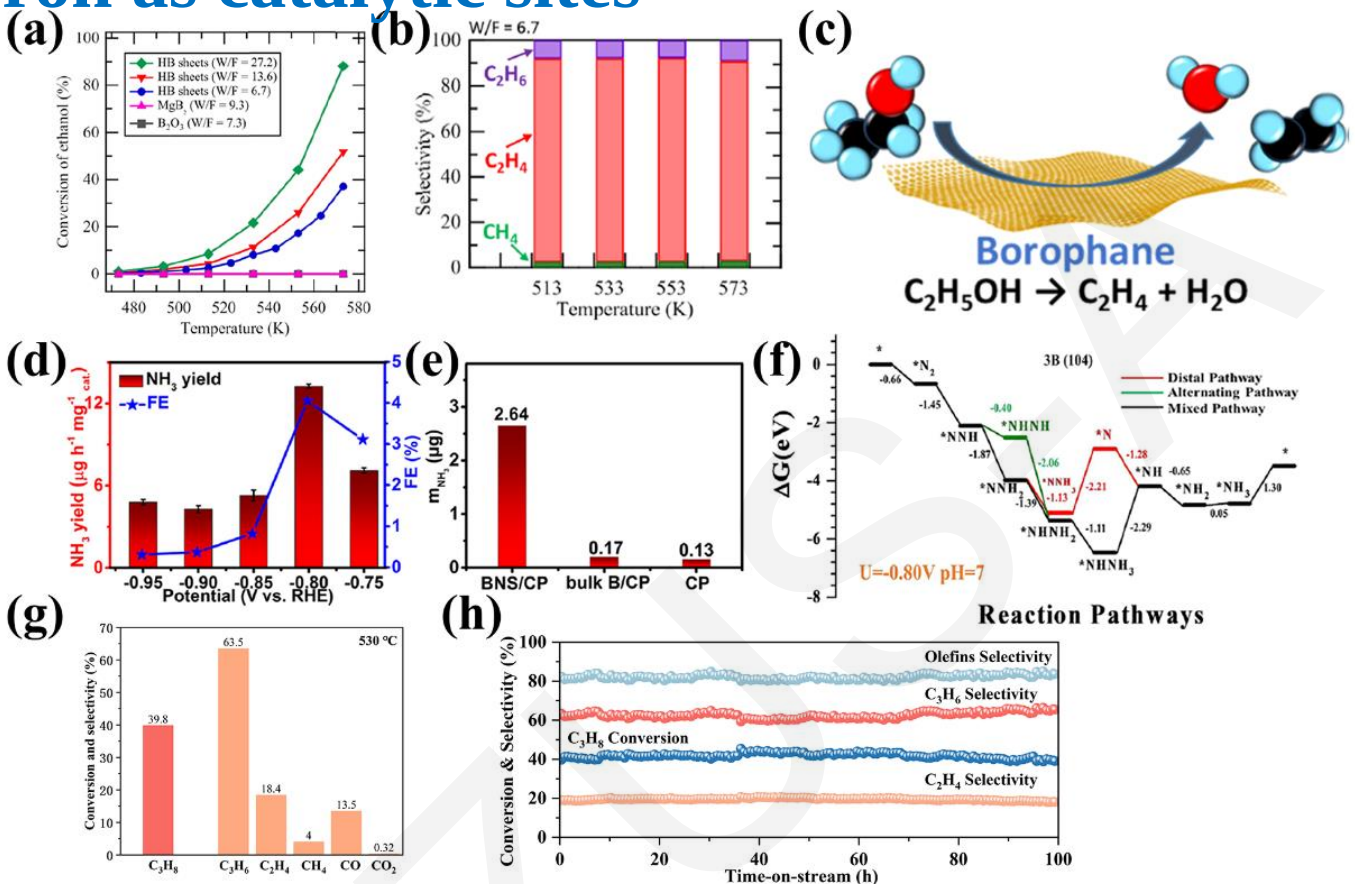


Fig. 4 (a) Ethanol conversion of HB sheets, MgB_2 and B_2O_3 at different temperatures. (b) Selectivity of ethanol reforming by HB as a function of temperature. (c) Schematic illustration of ethanol dehydration on HB sheets. (a-c) Reprinted from (Fujino, et al., 2019) (Copyright 2019, with permission from the American Chemical Society). (d) NH_3 yields and Faraday Efficiencies (FE) for BNS/CP under the corresponding potential. (e) Yields of NH_3 produced with different electrodes at -0.8 V after 2 h of electrolysis. (f) Free-energy diagram of NRR on the B(104) surface. (d-f) Reprinted from (Zhang, et al., 2019) (Copyright 2019, with permission from the American Chemical Society). (g) Catalytic performance of Mg-BNS at 530°C. (h) Stability test of Mg-BNSs at 530°C. (g-h) Reprinted from (Zhang, et al., 2024) (Copyright 2024, with permission from the Royal Society of Chemistry).

2D boron as catalytic supports

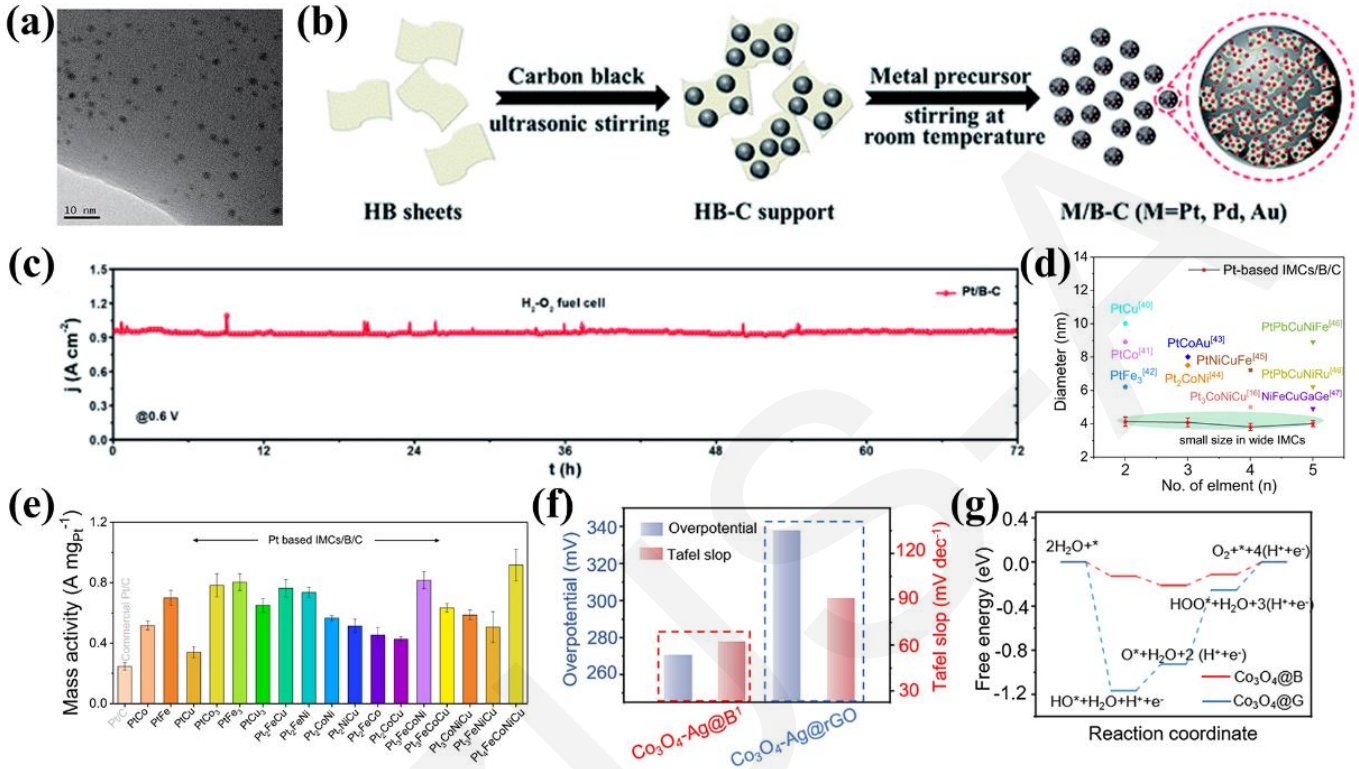


Fig. 5 (a) TEM image of Cu nanoparticles on a HB nanosheet. Reprinted from (Ito, et al., 2020) (Copyright 2020, with permission from The Chemical Society of Japan). (b) Schematic illustration of the synthetic process of M/B-C. (c) H_2-O_2 fuel cell durability test of Pt/B-C at 0.6 V for 72 h. (b-c) Reprinted from (Gao, et al., 2020) (Copyright 2020, with permission from the Royal Society of Chemistry. (d) Comparison of intermetallic alloy size between Pt-based intermetallic compounds with the reported works. (e) The mass activity of commercial Pt/C and Pt-M/B/C for ORR. (d-e) Reprinted from (Zeng, et al., 2023) (Copyright 2023, with permission from Nature Research). (f) The overpotentials and Tafel slopes to achieve 10 mA cm^{-2} for Co_3O_4-Ag@B and Co_3O_4-Ag@rGO catalysts. (g) Reaction free energy diagram for OER on Co_3O_4/B and Co_3O_4/graphene. (f-g) Reprinted from (Saad, et al., 2021) (Copyright 2021, with permission from Elsevier)

Summary and Perspective

To conclude, 2D boron is a treasure trove for energy catalysis. Its potential for the advanced catalytic systems has just emerged but has been underpinned by recent demonstrative works. Its sustainable development and further exploitation will be contingent on judicious design of the materials synthetic methods that likely involve the facile and productive top-down approaches. Bearing both the functional groups and metal sites that can participate in the reactions, the obtained boron nanosheets may be excellent options for boosting catalytic performance.

JZUS-A